FXR Regulates Liver Repair after CCl_4-Induced Toxic Injury

Zhipeng Meng, Yandong Wang, Lin Wang, Wen Jin, Nian Liu, Hao Pan, Lucy Liu, Lawrence Wagman, Barry M. Forman, and Wendong Huang

Department of Gene Regulation and Drug Discovery (Z.M., Y.W., L.Wan., W.J., N.L., H.P., L.L., B.M.F., W.H.) and Department of Surgery (L.Wag.), Liver Tumor Program, Beckman Research Institute, City of Hope National Medical Center, Duarte, California 91010

Liver repair is key to resuming homeostasis and preventing fibrogenesis as well as other liver diseases. Farnesoid X receptor (FXR, NR1H4) is an emerging liver metabolic regulator and cell protector. Here we show that FXR is essential to promote liver repair after carbon tetrachloride (CCl_4)-induced injury. Expression of hepatic FXR in wild-type mice was strongly suppressed by CCl_4 treatment, and bile acid homeostasis was disrupted. Liver injury was induced in both wild-type and $FXR^{-/-}$ mice by CCl_4, but $FXR^{-/-}$ mice had more severe defects in liver repair than wild-type mice. $FXR^{-/-}$ livers had a decreased peak of regenerative DNA synthesis and reduced induction of genes involved in liver regeneration. Moreover, $FXR^{-/-}$ mice displayed increased mortality and enhanced hepatocyte deaths. During the early stages of liver repair after CCl_4 treatment, we observed overproduction of TNFα and a strong decrease of phosphorylation and DNA-binding activity of signal transducer and activator of transcription 3 in livers from $FXR^{-/-}$ mice. Exogenous expression of a constitutively active signal transducer and activator of transcription 3 protein in $FXR^{-/-}$ liver effectively reduced hepatocyte death and liver injury after CCl_4 treatment. These results suggest that FXR is required to regulate normal liver repair by promoting regeneration and preventing cell death. (***Molecular Endocrinology* 24: 886–897, 2010**)

The liver is the major organ to manage the detoxification of both exogenous and endogenous insults and therefore is constantly exposed to injury agents. Liver repair is an intrinsic defense mechanism to protect liver from injury. Impaired liver repair will lead to fibrogenesis and cirrhosis, which may eventually result in either liver failure or hepatocellular carcinoma. Many genes and pathways have been identified to regulate liver repair.

Farnesoid X receptor (FXR) belongs to the nuclear hormone receptor superfamily and is highly expressed in liver, intestine, kidney, and adrenal glands (1). FXR is the primary bile acid (BA) receptor that acts as a master regulator of BA homeostasis (2–7). BAs are end products of cholesterol catabolism and are essential for normal absorption of cholesterol, lipids, and fat-soluble vitamins by the intestine (8). BAs are synthesized in the liver and stored in the gall bladder. They are secreted into the intestine after food intake, but most BAs (95%) are reabsorbed and transported back to the liver through the portal vein. This system is known as enterohepatic circulation. The levels of BAs need to be tightly controlled due to their surfactant properties and hepatotoxicity at high doses. Accumulation of BAs in the liver, which may occur during intrahepatic cholestasis of pregnancy (9), or inherent diseases such as progressive familial intrahepatic cholestasis 1 and 2 (PFIC1 and PFIC2) (10–12), results in hepatocellular apoptosis and necrosis, thereby promoting liver fibrosis and cirrhosis (13).

To prevent the BA hepatotoxicity, liver has an intrinsic mechanism with which to sense and control BA levels by

ISSN Print 0888-8809 ISSN Online 1944-9917
Printed in U.S.A.

doi: 10.1210/me.2009-0286 Received July 20, 2009. Accepted February 4, 2010.
First Published Online March 8, 2010

Abbreviations: ALT, Alanine aminotransferase; BA, bile acid; BDL, bile duct ligatior BrdU, 5-bromo-2′-deoxy-uridine; CA, cholic acid; FXR, farnesoid X receptor; GCDCA, glycochenodeoxycholic acid; H&E, hematoxylin and eosin; JAK, Janus kinase; MRP, multidrug-resistant protein; NF-κB, nuclear factor-κB; PFIC, progressive familial intrahepatic cholestasis; PH, partial hepatectomy; SHP, small heterodimer partner; STAT3, signal transducer and activator of transcription 3.

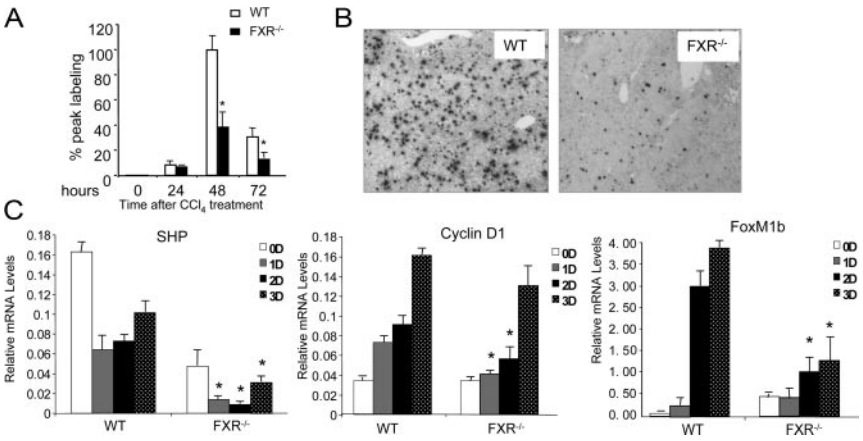

FIG. 1. Defective liver regeneration in $FXR^{-/-}$ mice after CCl_4-induced liver injury. A, The BrdU-positive liver cells were counted as described previously (17). *, $P < 0.05$. B, Representative images of BrdU staining of liver tissue from wild-type (WT) and $FXR^{-/-}$ mice on the second day after CCl_4 treatment. C, Gene expression analysis of *SHP*, *FoxM1b*, and *CyclinD1* by quantitative real-time PCR. *, $P < 0.05$.

FXR. In PFIC1 patients, the decreased FXR activity is regarded as one of the primary reasons of the pathogenesis (10). Functional variants of FXR are detected in patients with intrahepatic cholestasis of pregnancy (9). Function of FXR in cholestasis is further clarified by the synthetic FXR agonist, GW4064, which prevents cholestatic liver diseases induced by bile duct ligation (BDL) through down-regulating BA synthetic genes and increasing expression of BA transport genes (14). Another FXR agonist, 6-ethyl-chenodeoxycholic acid, effectively suppresses the liver fibrosis caused by BDL in rats (13). Knockout of small heterodimer partner (SHP), the primary target gene of FXR, leads to increased liver damage by BDL (15), which also supports the roles of FXR in liver protection. In a recent study, $FXR^{-/-}$ mice were shown to be more susceptible to α-naphthyl isothiocyanate-induced acute intrahepatic cholestatic liver injury (16). However, the role of FXR in liver repair after injury is still not very clear.

We previously showed that FXR was required for normal liver regeneration after injury in a 70% partial hepatectomy (PH) model by promoting proliferation of liver cells (17). Rodents treated with CCl_4 are widely used to study the mechanisms of toxin-induced liver injury (18, 19). CCl_4-induced hepatic injury is characterized by centrilobular necrosis and followed by hepatic fibrosis, which recapitulates drug-induced acute liver failure. Compared with 70% PH model, which leaves the remaining 30% of the liver intact, CCl_4 injection model of liver injury and repair is closer to the clinical liver injury cases with simultaneous severe hepatocyte deaths and acute cholestasis. Therefore, we use this model to ask: 1) whether FXR is also required for normal liver repair in response to CCl_4-induced hepatic cell deaths as it does in the 70% PH surgical model; 2) whether CCl_4-induced hepatic necrosis and apoptosis potentially disrupt BA homeostasis, and whether this disruption will interfere with the normal liver repair process.

Results

Defective liver regeneration in $FXR^{-/-}$ mice after CCl_4 treatment

Wild-type and $FXR^{-/-}$ mice were injected ip with CCl_4 in corn oil (750 μl/kg body weight) or the same volume of corn oil alone as vehicle control. First we determined the expression levels of *CYP2E1*, which is the primary cytochrome P450 that catalyzes CCl_4 metabolism. We did not observe a significant difference in the levels of *CYP2E1* mRNA between wild-type and $FXR^{-/-}$ mice after CCl_4 injection (Supplemental Fig. 1A published on The Endocrine Society's Journals Online web site at http://mend.endojournals.org). However, $FXR^{-/-}$ mice exhibited greater mortality (~20%, three of 17 mice) 3 d after CCl_4 treatment (Supplemental Fig. 1B), suggesting that FXR may be important for preventing liver failure-induced death.

Liver repairs itself by regenerating the survived cells. Therefore, we compared the abilities of $FXR^{-/-}$ and wild-type hepatocytes to proliferate after CCl_4-induced liver injury. $FXR^{-/-}$ mice had a severe reduction of hepatocyte proliferation compared with the wild-type controls (Fig. 1). There were significantly fewer 5-bromo-2′-deoxy-uridine (BrdU) positive hepatocytes in the $FXR^{-/-}$ livers compared with the wild-type controls, starting from the second day after CCl_4 injection (Fig. 1, A and B). Consistent with these data, there were also significantly fewer mitotic indexes in the $FXR^{-/-}$ livers (data not shown). These results confirm an essential role of FXR in promoting liver regeneration after toxin-induced injury.

Gene expression in the liver after CCl_4-induced injury was examined by quantitative real-time PCR. Expression of *SHP*, the major FXR target gene in BA metabolism, was suppressed by CCl_4 treatment in the first 2 d, indicating that FXR activation may be affected by CCl_4 treatment. In the $FXR^{-/-}$ mice, the SHP mRNA level was even more decreased, but recovered on the third day as the wild-type controls, indicating that expression of SHP during the liver injury was also modulated by FXR-independent pathways. Expression of the cell cycle gene, *Cyclin D1*, was reduced in the $FXR^{-/-}$ livers. Similarly, the induction of *FoxM1b*, a previously identified target gene regulated by FXR during liver regeneration, was significantly reduced in the $FXR^{-/-}$ mice after CCl_4-induced liver injury (Fig. 1C).

Increased hepatocyte death and liver injury in FXR$^{-/-}$ mice after CCl_4 treatment

BAs are synthesized specifically from cholesterol in the liver and subsequently excreted into bile. We observed a significant increase of serum BA levels after CCl_4 injection in the wild-type mice, which suggests that liver injury caused by CCl_4 may impair enterohepatic circulation and BA homeostasis (Fig. 2A). Compared with the wild-type controls, the levels of serum BAs in the FXR$^{-/-}$ mice were 2-fold higher at all time points. Consistently, 1 d after injection of CCl_4, there was significantly higher level of serum alanine aminotransferase (ALT) in the FXR$^{-/-}$ mice, but both genotypes reached a peak of similar ALT levels on the second day after injection (Fig. 2B). CCl_4-induced liver injury is usually accompanied by increased hepatocyte apoptosis. Therefore, we compared the amount of apoptotic hepatocytes in the wild-type and the FXR$^{-/-}$ livers. TUNEL staining indicated that significantly greater numbers of apoptotic hepatocytes were present in the FXR$^{-/-}$ mice as compared with the wild-type controls (Fig. 2, C and D), which was further confirmed by higher levels of cleaved Caspase 3 in the FXR$^{-/-}$ livers (Fig. 2E). CCl_4 also directly leads to severe necrosis in the liver. Hematoxylin and eosin (H&E) staining showed more necrotic areas in the FXR$^{-/-}$ livers than in the wild-type controls (Fig. 2F). These results demonstrate that liver injury disrupts BA homeostasis, and FXR$^{-/-}$ mice are more susceptible to CCl_4-induced liver injury.

Intrahepatic cholestasis of FXR$^{-/-}$ mice after CCl_4 treatment

To further understand the effects of FXR loss on the increased BA flux, we evaluated the hepatic total BAs in the wild-type and the FXR$^{-/-}$ mice. Hepatic BAs began to accumulate in liver 24 h after the CCl_4 treatment and were lowered to normal levels on the third day in the wild-type mice (Fig. 3A). In contrast, the intrahepatic BA level was sharply increased in the FXR$^{-/-}$ mice during the acute phase and kept at a much higher level than that in wild-type controls until 7 d after the treatment. The expression of the major BA synthetic enzyme *CYP7A1* was

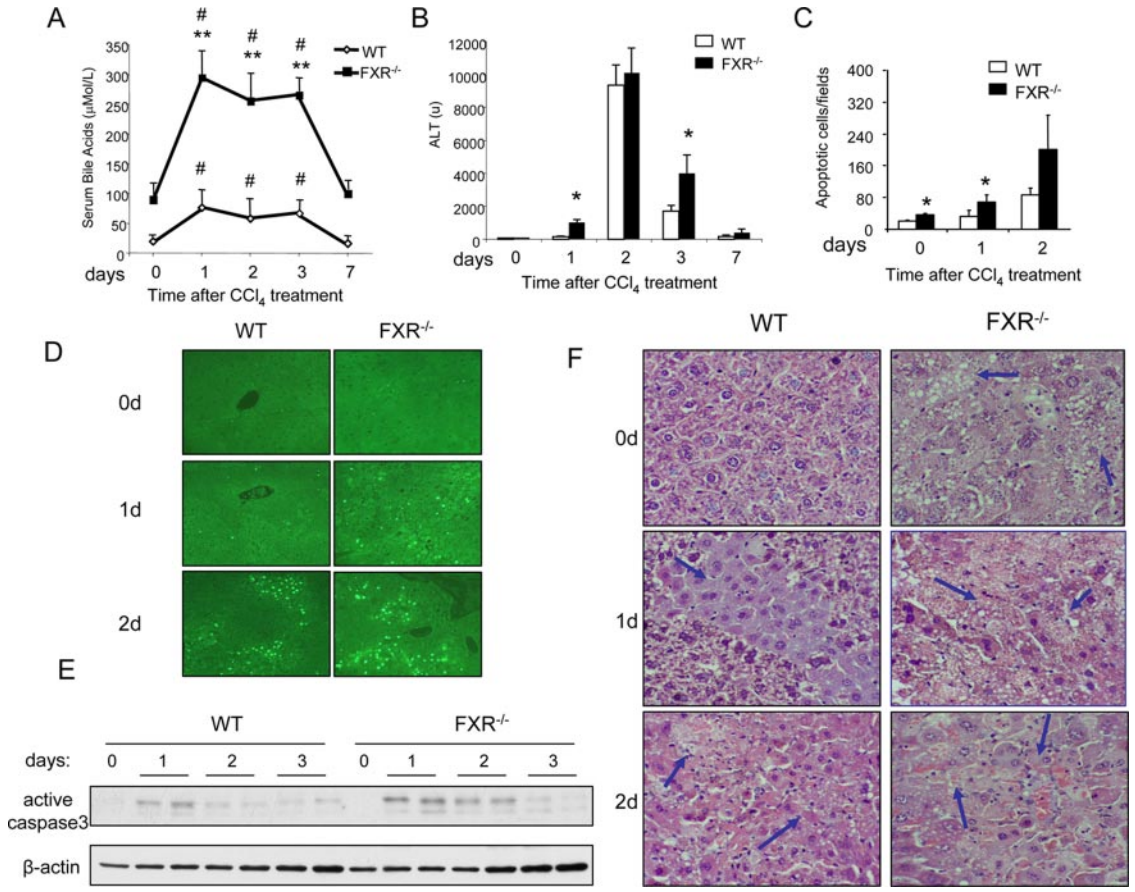

FIG. 2. Increased hepatocyte apoptosis and liver injury in FXR$^{-/-}$ livers after CCl_4 treatment. A, Serum BA levels in wild-type (WT) or FXR$^{-/-}$ mice after CCl_4 treatment. **, FXR$^{-/-}$ *vs.* WT, $P < 0.01$; #, serum BAs of FXR$^{-/-}$ mice treated with CCl_4 *vs.* serum BAs of FXR$^{-/-}$ mice at time zero. B, Serum ALT levels in WT or FXR$^{-/-}$ mice after CCl_4 treatment. *, $P < 0.05$. C, Quantification of apoptotic hepatocytes. *, $P < 0.05$. D, Terminal deoxynucleotide transferase-mediated dUTP nick end labeling staining of liver sections from WT and FXR$^{-/-}$ mice after CCl_4 treatment (0, 1, or 2 d after treatment). E, Caspase 3 activation after CCl_4 injection in WT and FXR$^{-/-}$ mice. F, H&E staining of liver tissue sections from WT and FXR$^{-/-}$ mice after CCl_4 treatment. *Arrows* indicate necrosis areas.

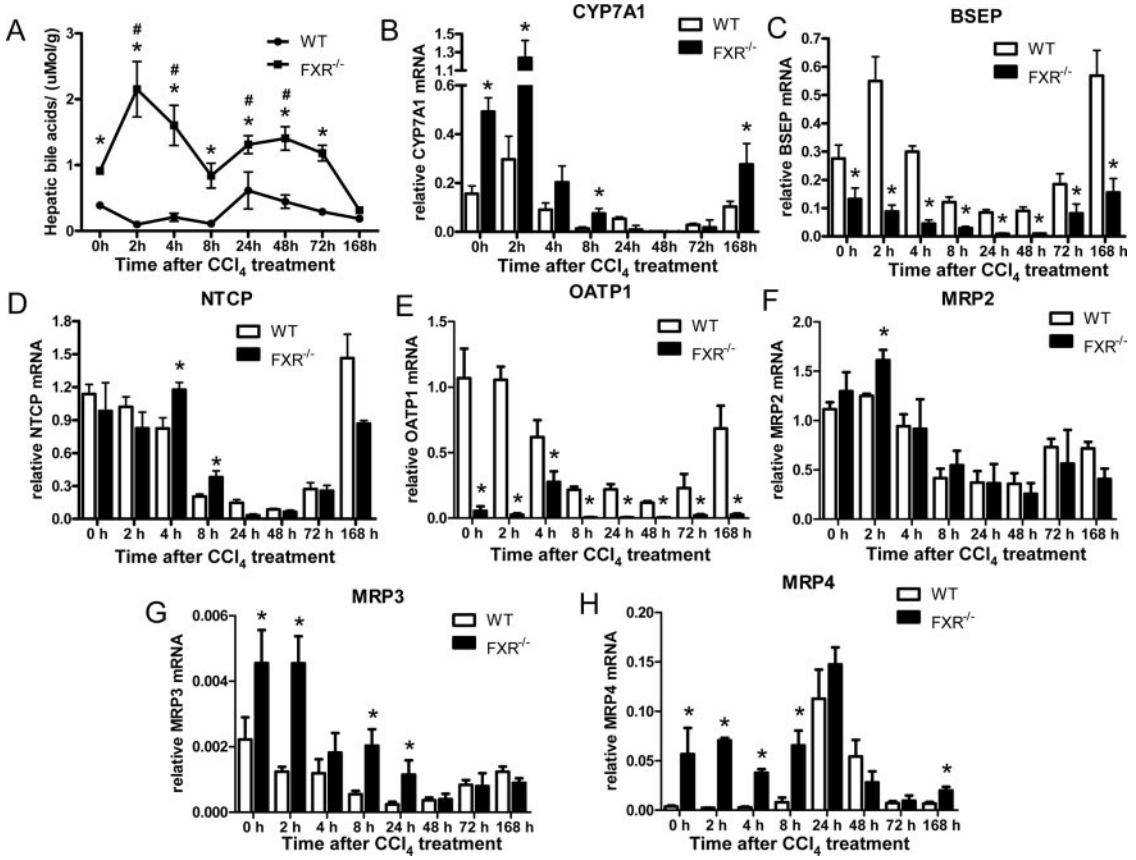

FIG. 3. Intrahepatic cholestasis of $FXR^{-/-}$ mice after CCl_4 treatment. A, Hepatic BAs were measured as described in *Materials and Methods*. *, $FXR^{-/-}$ *vs.* wild type (WT), $P < 0.05$; #, hepatic BAs of $FXR^{-/-}$ mice treated with CCl_4 *vs.* hepatic BAs of $FXR^{-/-}$ mice at zero time. B–H, Quantitative real-time PCR analysis of CYP7A, BSEP, NTCP, OATP1, and MRP2/3/4 expression. The quantity of mRNA was normalized using the internal standard, m36B4. *, $P < 0.05$.

significantly increased in the $FXR^{-/-}$ mice at the second hour whereas the *CYP7A1* in the wild-type mice was not greatly increased compared with the nontreated control (Fig. 3B). *BSEP* is responsible for the transport of taurocholate and other cholate conjugates from hepatocytes to the bile, and its expression is activated by FXR (20). The early activation of *BSEP* transcription was not seen in the $FXR^{-/-}$ mice, and the expression levels were less than 50% of those in the wild-type controls at most of the time points (Fig. 3C). FXR reduces the BAs inside the hepatocytes also by suppressing *NTCP* expression. This suppression was slightly impaired in the $FXR^{-/-}$ mice in the acute phase after liver injury (Fig. 3D). The expression of *OATP1*, the organic anion-transporting peptide that helps hepatocytes uptake BAs together with *NTCP* at the basolateral membrane of hepatocytes, was decreased by CCl_4 treatment in wild-type mice. The $FXR^{-/-}$ mice showed much lower levels of *OATP1* expression in liver both before CCl_4 treatment and during liver repair (Fig. 3E). Intrahepatic cholestasis also changes expression of ATP-binding cassette transporters [multidrug-resistant proteins (MRPs)]. Although MRP2 was reported as a FXR target gene (21), its expression in the $FXR^{-/-}$ mice was not very different from that of the wild-type controls (Fig. 3F). Similar to the BDL cholestasis model of $FXR^{-/-}$ mice, MRP3 and MRP4 were up-regulated in the $FXR^{-/-}$ mice via a FXR-independent manner (Fig. 3, G and H). In summary, due to the differentiated expression of *CYP7A1*, *BSEP*, and *NTCP*, $FXR^{-/-}$ mice developed more severe intrahepatic cholestasis despite their lower levels of *OATP1* and adaptive up-regulation of *MRP3/4*.

Exogenous overexpression of a constitutively active FXR suppressed liver injury after CCl_4 treatment

Of interest, the expression of FXR was strongly suppressed after CCl_4 treatment (Fig. 4A), raising the question of whether it is the decreased FXR expression that contributes to liver injury. Therefore we infected the wild-type mice with an adenovirus expressing a constitutively active form of FXR, FXR-VP16, as described previously to test whether FXR overexpression rescues CCl_4-induced liver injury (Supplemental Fig. 2A) (22). Compared with the controls infected with adenovirus expressing VP16 only, the mice infected with FXR-VP16 showed increased expression of *SHP* and reduced expression of

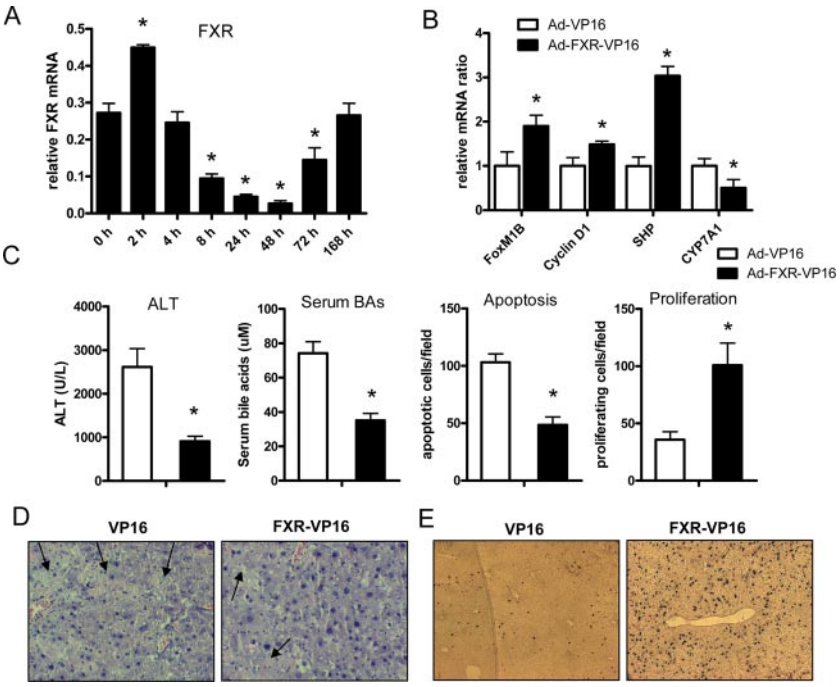

FIG. 4. Overexpression of a constitutively active FXR (FXR-VP16)-suppressed liver injury caused by CCl_4. A, mRNA levels of FXR at the different time points after CCl_4 injection. *, One-way ANOVA test followed by a *post hoc* test (Dunnett's Multiple Comparison Test) compared with control group, $P < 0.05$. B, Gene expression analysis in the wild-type mice infected by adenovirus (Ad)-expressing FXR-VP16 or VP16 alone 40 h after CCl_4 treatment. C, Serum ALT, serum BAs, Terminal deoxynucleotide transferase-mediated dUTP nick end labeling, and BrdU staining in the mice treated with FXR-VP16 adenovirus or VP-16 adenovirus 40 h after CCl_4 treatment. *, $P < 0.05$. D, Representative figures of H&E staining. *Arrows* indicate necrosis. E, Representative figures of BrdU staining.

CYP7A1 40 h after CCl_4 treatment (Fig. 4B). Two genes regulating the cell cycle, *FoxM1B* and *Cyclin D1*, were increased by FXR-VP16 infection (Fig. 4B). Overexpression of FXR-VP16 effectively reduced serum BA levels and ALT levels and rescued apoptosis and necrosis of the hepatocyte after CCl_4 administration (Fig. 4, C and D). The proliferation of the hepatocytes, as shown by BrdU staining, was simultaneously increased (Fig. 4, C and E).

Reduced signal transducer and activator of transcription 3 (STAT3) activities in $FXR^{-/-}$ mice during early time points after CCl_4 treatment

Hepatocytes normally exist in a highly differentiated quiescent G_0 phase. Upon injury, the remaining hepatocytes are primed by protooncogenes such as c-*fos*, c-*jun*, and c-*myc*, the cytokines, *TNFα* and *IL-6*, and acute phase response factors including nuclear factor-κB (NF-κB) and STAT3 (23).

The induction of c-*jun* and c-*fos* is similar between the $FXR^{-/-}$ mice and the wild-type mice (Fig. 5A). However, the $FXR^{-/-}$ mice exhibited surprisingly high levels of c-*myc* induction (Fig. 5A). Although certain level of c-*myc* expression can promote the initiation of hepatocyte proliferation, the overactivation of c-*myc* may lead to cellular senescence and apoptosis in the liver (24).

CCl_4 preferentially induces *TNFα* production in its early phase (25). In the wild-type mice, *TNFα* was induced and achieved a peak at the second hour, and its expression level was still maintained at the eighth hour. $FXR^{-/-}$ mice had preexisting high levels of *TNFα* and the expression was further enhanced by CCl_4 and almost 2-fold higher than that in wild-type livers (Fig. 5B). The exaggerated *TNFα* might result in overexpression of c-*myc* and contribute to the increased necrosis and apoptosis in $FXR^{-/-}$ livers. *IL-6* is a cytokine that plays a mainly protective role during liver injury. The induction of this cytokine was seen as early as the second hour, and the magnitude of induction could achieve a higher level on the eighth hour. However, no significant difference of *IL-6* production in the acute phase was seen between the wild-type and the $FXR^{-/-}$ mice (Fig. 5B).

However, we observed a dramatically reduced DNA-binding activity of STAT3 in the $FXR^{-/-}$ livers (Fig. 6A). Whereas STAT3 activity was strongly up-regulated in the wild-type livers 2 h after CCl_4 injection, this induction was much less in the $FXR^{-/-}$ livers. The result was further confirmed by Western blotting, which showed less STAT3 tyrosine phosphorylation in the $FXR^{-/-}$ livers (Fig. 6B). In addition, the STAT3 phosphorylation at later time points, which correlates with the initiation of the second round of the hepatocyte proliferation, was delayed in the $FXR^{-/-}$ livers until 2 d after the treatment, but $FXR^{-/-}$ mice showed greatly enhanced hepatic STAT3 phosphorylation at 3 d after the treatment. We also investigated NF-κB activation by measuring the nuclear translocation of p65, a catalytic subunit of NF-κB. There was a comparable increase in the levels of p65 in the nucleus of the wild-type and the $FXR^{-/-}$ livers after CCl_4 injection (Fig. 6C). To further confirm the defective STAT3 activation in the $FXR^{-/-}$ livers, we measured the expression of two STAT3 target genes *Bcl-xl* and *SOCS3* (26, 27) in the acute responses after CCl_4 treatment. Consistent with the STAT3 DNA-binding activity pattern, induction of *Bcl-xl* and *SOCS3* was either decreased or delayed in the $FXR^{-/-}$ livers compared with induction of these two genes in the wild-type livers (Fig. 6D). The lower expression of the antiapoptotic gene, *Bcl-xl,* might contribute to the enhanced cell deaths in the $FXR^{-/-}$ livers.

We restored FXR activities in $FXR^{-/-}$ mice by introducing the adenovirus expressing FXR-VP16. Adenovi-

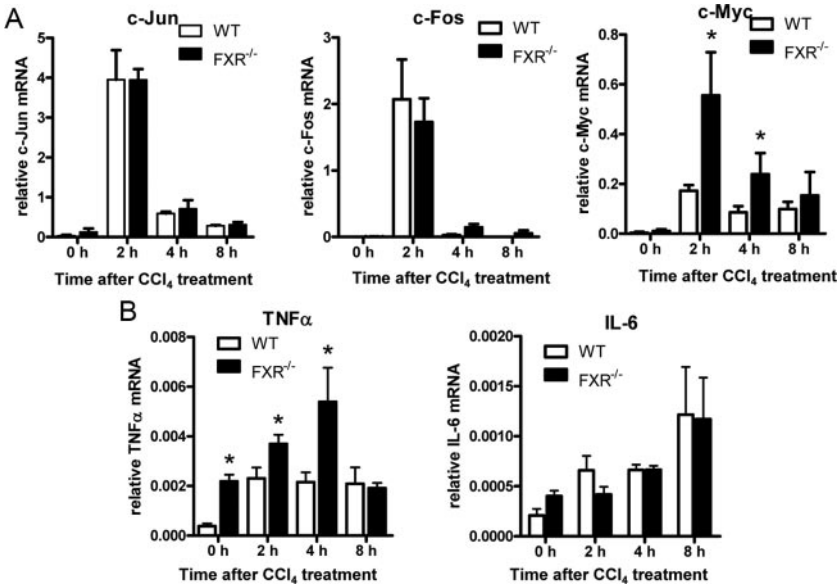

FIG. 5. Expression analysis of early response genes in liver tissues from CCl_4-treated wild-type (WT) and $FXR^{-/-}$ mice. Total hepatic RNA was prepared from wild-type and $FXR^{-/-}$ mice and subjected to quantitative real-time PCR analysis. A, Acute phase protooncogenes c-*jun*, c-*fos*, and c-*myc*. B, Inflammatory cytokines TNFα and IL-6. The quantity of mRNA was normalized using the internal standard, m36B4. *, $P < 0.05$.

rus expressing FXR-VP16 itself lowered basal levels of serum ALT and BAs of $FXR^{-/-}$ mice compared with control adenovirus that expressed VP16 alone (Supplemental Fig. 2B). The FXR-VP16 adenovirus restored the phosphorylation of STAT3 in the acute phases after CCl_4 treatment (Fig. 6E) as well as promoted the expression of the STAT3 target gene *SOCS3* (Fig. 6F) without changing hepatic IL-6 expression (Supplemental Fig. 3A). These results suggest a role of FXR for normal STAT3 activation in the acute phase of liver injury.

High levels of BAs suppress STAT3 phosphorylation during liver regeneration

We then tested whether FXR activation directly affected the STAT3 phosphorylation in primary hepatocytes. FXR ligand GW4064 was not able to initiate STAT3 phosphorylation or prolong IL-6-induced STAT3 phosphorylation of the wild-type primary hepatocytes although the effectiveness of GW4064 on FXR activation was shown by the increased ERK1/2 phosphorylation (28) (Fig. 7A). Furthermore, no significant difference of IL-6-induced STAT3 phosphorylation was observed between the wild-type and the $FXR^{-/-}$ primary hepatocytes (Fig. 7B).

A major deregulation in the $FXR^{-/-}$ mice was the sustained higher levels of BAs in serum and liver. Therefore, we tested whether high BA levels would affect STAT phosphorylation. We first fed the mice with a 4% cholestyramine (Resin) diet to reduce BA levels in $FXR^{-/-}$ mice as we previously described (17). Indeed, we observed a reduced suppression of STAT3 phosphorylation after CCl_4 treatment by Resin feeding compared with the controls (Fig. 7C). On the other hand, when we fed the wild-type mice with a 1% cholic acid (CA) diet, we observed a suppression of STAT3 phosphorylation after CCl_4 treatment (Fig. 7C and Supplemental Fig. 4A). This suppression of hepatic STAT3 phosphorylation by 1% CA feeding was even more prominent in the wild-type mice with 70% PH (Fig. 7C and Supplemental Fig. 4B). These results suggest that high levels of BAs contribute to the reduced STAT3 phosphorylation in the $FXR^{-/-}$ livers after CCl_4 treatment. However, neither Resin- nor CA-containing diet altered hepatic IL-6 expression (Supplemental Fig. 3, B–D).

BAs are known to directly modulate phosphorylation of STAT3 by affecting its upstream components (29, 30). It was reported that certain hydrophobic BAs such as glycochenodeoxycholic acid (GCDCA) down-regulated IL-6-induced STAT3 phosphorylation through both gp130-dependent and p38α-dependent pathways. Treatment of GCDCA to cultured rat primary hepatocytes caused caspase-mediated gp130 degradation (30). Therefore, we compared gp130 protein levels between the 1% CA-containing diet feeding mice and the mice fed with the normal diet after 70% PH, and between the $FXR^{-/-}$ mice and the wild-type mice treated with CCl_4. However, no significant difference was observed (Supplemental Figs. 4C and 7D). The levels of p38α phosphorylation between the two groups were comparable (Fig. 7D). Furthermore, there was no difference in the induction of p38α phosphorylation between 1% CA-containing diet-fed mice and the wild-type controls (Supplemental Fig. 4C).

STAT3 pathways are known to be directly regulated mainly through another two upstream components, Janus kinase (JAK)1 and JAK2, the phosphorylated forms of which, in turn, phosphorylate STAT3 (23, 31). We found that phosphorylation of both JAK1 and JAK2 was impaired in the $FXR^{-/-}$ mice. Thus we speculated whether BAs affected phosphorylation of JAK1 and JAK2 through a gp130- and p38α-independent pathway. Indeed, 4% Resin-containing diet effectively restored phosphorylation of JAK1 and JAK2 in the $FXR^{-/-}$ mice after CCl_4 treatment (Fig. 7E). In addition, 1% CA-containing diet greatly reduced phosphorylation of both JAK1 and JAK2 in the wild-type mice after 70% PH (Fig. 7F). Furthermore, we observed that the CA-containing diet would augment CCl_4-induced

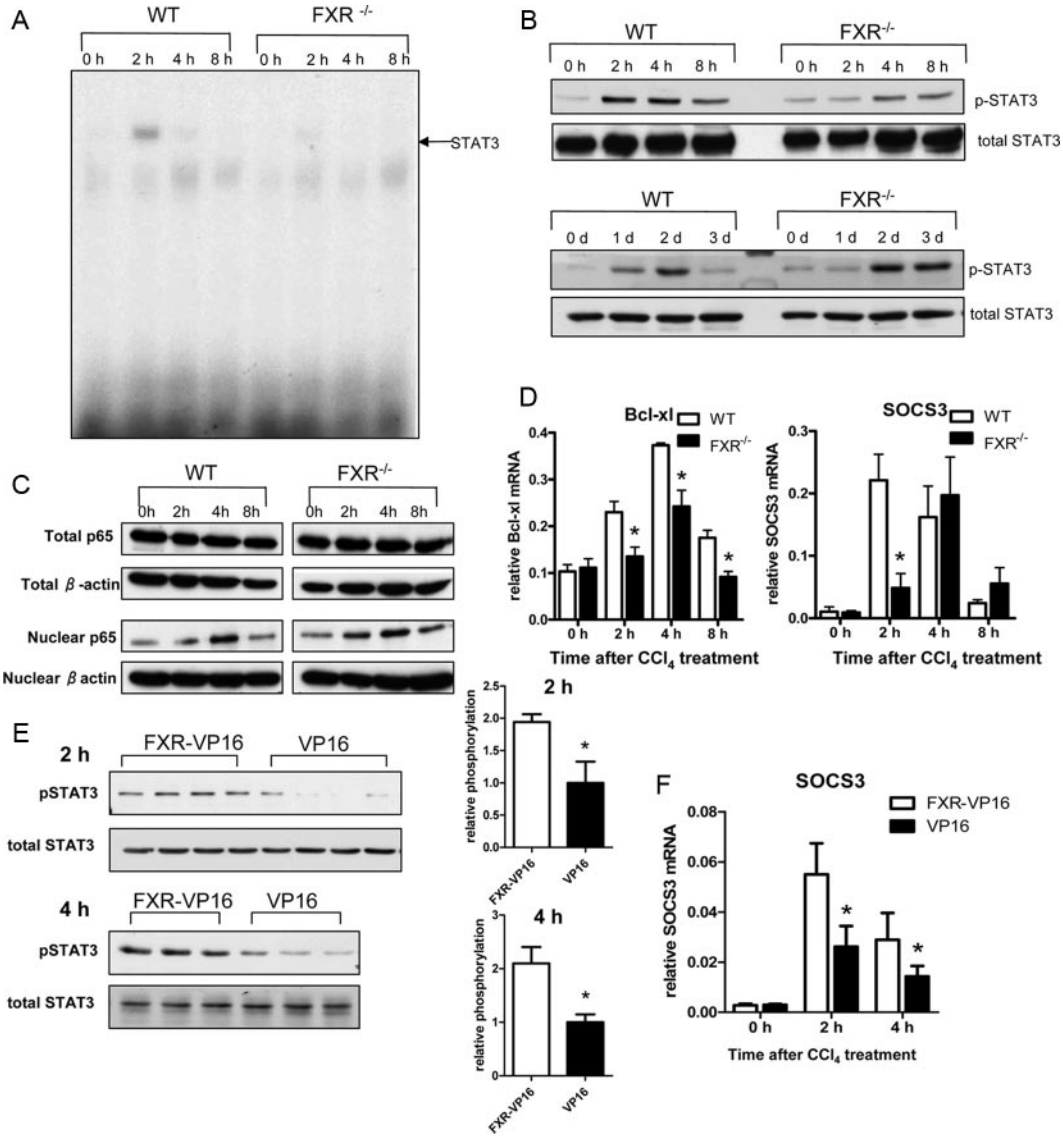

FIG. 6. Impaired STAT3 activation after CCl_4 treatment in $FXR^{-/-}$ mice. A, EMSA analysis of nuclear proteins (8 μg) extracted from pooled livers of four to six mice at the indicated times after CCl_4 injections. *Arrow* indicates STAT3 homodimer. B, Western blot analysis of total protein extracts (30 μg) from the same liver samples as in panel A and the samples collected at later time points (1, 2, and 3 d). Blots were probed for STAT3 Tyr705 phosphorylation or total STAT3 protein levels using corresponding antibodies. C, Immunoblot analysis of total liver lysates or nuclear liver lysates (30 μg) from CCl_4-treated mice at the indicated time points after treatment. Blots were probed with anti-p65 and anti-β-actin antibody. D, mRNA levels of STAT3 target genes Bcl-xl and SOCS3. *, $P < 0.05$. E, Immunoblot of phospho-STAT3 in the $FXR^{-/-}$ mice infected with adenovirus. F, Real-time PCR analysis of SOCS3 in the $FXR^{-/-}$ mice infected with adenovirus. *, $P < 0.05$. SOCS, Suppressor of cytokine signaling; WT, wild type.

liver injury and impair liver repair whereas the Resin-containing diet slightly reduced CCl_4-induced liver injury and help liver repair (Supplemental Fig. 5, A–F).

Exogenous overexpression of a constitutively active STAT3 suppressed liver injury in $FXR^{-/-}$ mice after CCl_4 treatment

To better understand the specific roles of STAT3 in mediating the effects of FXR on hepatocyte survival, we expressed a constitutively active STAT3 (STAT3C) in $FXR^{-/-}$ livers via hydrodynamic tail vein injection (32). Hydrodynamic injection resulted in STAT3 protein expression in liver and enhanced expression of STAT3 target gene Bcl-xl (Fig. 8A). We then treated the mice with CCl_4 (750 μl/kg) 1 d after the hydrodynamic transfection. Exogenous overexpression of STAT3C significantly reduced ALT levels, hepatocyte deaths, and liver injury after CCl_4 treatment in $FXR^{-/-}$ mice, whereas $FXR^{-/-}$ mice with the treatment of a control plasmid did not show different responses to CCl_4 compared with the mice receiving saline only (Fig. 8, B–F). These results demonstrate that diminished STAT3 activity in the $FXR^{-/-}$ livers after CCl_4 treatment may contribute to the enhanced hepatocyte deaths.

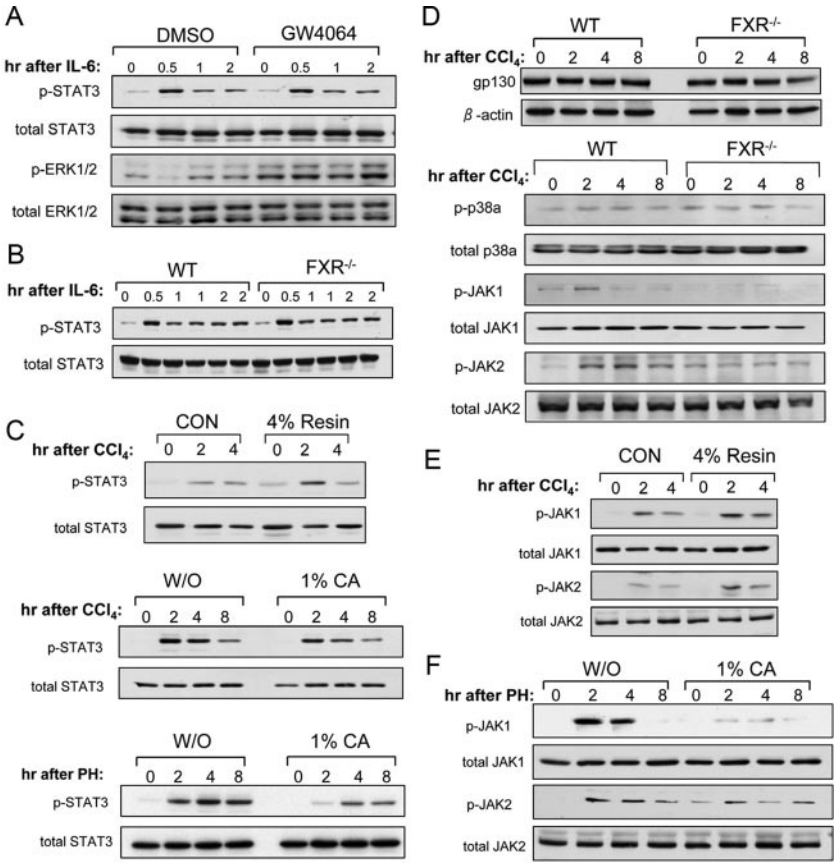

FIG. 7. High BA levels suppress STAT3 phosphorylation during liver regeneration. A, Primary hepatocytes from 8-wk-old wild-type mice were pretreated with 2 μM GW4064 or dimethylsulfoxide (DMSO) for 24 h and then treated with 10 ng/ml recombinant mouse IL-6. The total lysates from the hepatocytes were analyzed with Western blot. B, IL-6 induced STAT3 phosphorylation in wild-type (WT) and $FXR^{-/-}$ primary hepatocytes. C, Immunoblot analysis of STAT3 phosphorylation in total protein extracts pooled from livers of four to six $FXR^{-/-}$ mice prefed with a powdered diet supplemented with 4% cholestyramine (resin) or a control powdered diet (CON) for 5 d at the indicated time points after CCl_4 treatment, STAT3 phosphorylation in total protein extracts pooled from livers of four to six WT mice either received 1% CA feeding or normal diet (W/O) for 5 d and terminated at the indicated time points after CCl_4 treatment, and STAT3 phosphorylation in total liver protein extracts pooled from four WT mice that received the 1% CA-containing diet after 70% PH. D, Immunoblot analysis of gp130 protein levels, and phosphorylation of p38α, JAK1, and JAK2 in the liver of WT mice and $FXR^{-/-}$ mice after CCl_4 treatment. E, Immunoblot analysis of JAK1 and JAK2 phosphorylation in the $FXR^{-/-}$ mice fed with the 4% Resin-containing diet after CCl_4 treatment. F, Immunoblot analysis of phosphorylation of JAK1 and JAK2 in the livers of WT mice fed with normal diet (W/O) or 1% CA-containing diet after 70% PH.

Discussion

Liver repair is an intrinsic defense mechanism after injury. The impact of the liver metabolic pathways on liver injury and repair has not been well studied. We observe that CCl_4-induced liver injury disrupts the BA enterohepatic circulation and causes the accumulation of BAs in the liver. This may result from the repression of *FXR* expression and other key components involved in BA circulation such as the BA transporters. The suppression of FXR expression may be due to the increase of proinflammatory cytokines induced by strong liver injury (33). Interestingly, we observed a transient increase of FXR mRNA levels shortly after CCl_4 treatment. This could be due to the fact that FXR activation by increased BA flow up-regulates the transcription of FXR. BAs as well as FXR ligands, CDCA and GW4064, are shown to increase FXR mRNA levels (34, 35).

The key role of FXR in controlling BA levels after CCl_4 treatment was confirmed by $FXR^{-/-}$ mice that displayed severe cholestasis and exaggerated liver injury. Previous studies indicate that high levels of BAs can induce cell death and augment inflammatory cytokine production such as *TNFα* (Fig. 5B) (36). *TNFα* biosynthesis is required for liver repair after CCl_4 treatment, but overproduction of *TNFα* can induce more apoptosis mediated by TNF receptor/Fas-associates death domain pathways (37). Therefore, the uncontrolled inflammatory cytokine production due to high levels of BAs may contribute to the overall liver injury.

In this study, we also identify a specific effect of BAs on STAT3 activation. STAT3 signaling pathway, usually activated in the acute phase of liver injury, is a previously identified important pathway for survival and repair of liver cells. Here we show that overload of BAs caused by FXR deficiency leads to delayed responses of STAT3 to liver injury. Tyrosine phosphorylation of STAT3 was severely repressed in the $FXR^{-/-}$ livers in the acute phase of CCl_4-induced liver injury, although stronger responses of STAT3 were observed in the later stages of liver repair in $FXR^{-/-}$ mice. The compensatory hyperphosphorylation of STAT3 in the $FXR^{-/-}$ livers at the later stages was probably due to either the release of BA stress, such as compensatory exportation and conjugation of toxic hydrophobic BAs, or more aggravated inflammation caused by massive cell deaths in these mice, which may help to explain the accelerated recovery of $FXR^{-/-}$ mice after 3 d in the second round of hepatocyte cell cycling after injury (38).

We did not observe a direct effect of FXR on either basal or IL-6-induced STAT3 phosphorylation. Instead, we provide evidence that high levels of BAs in $FXR^{-/-}$ livers may result in reduced STAT3 phosphorylation. The BA levels are much higher in $FXR^{-/-}$ livers after CCl_4-induced liver injury than after 70% PH. It may suggest why we observed reduced STAT3 phosphorylation only

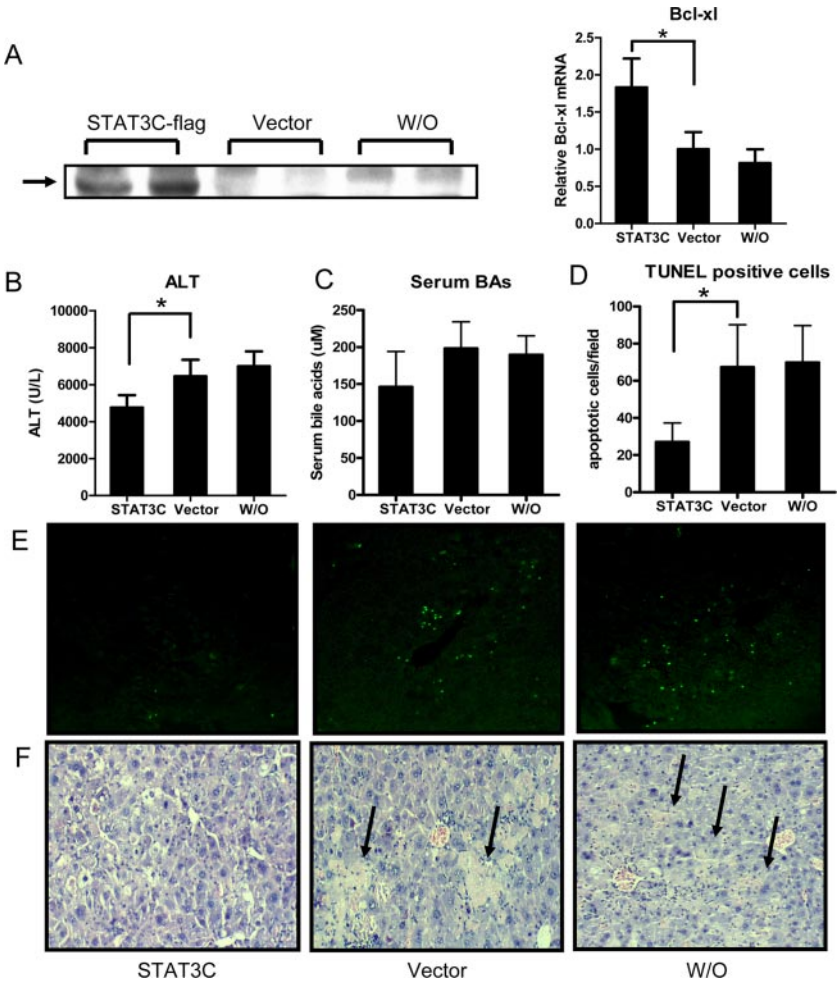

FIG. 8. Suppression of CCl_4-induced hepatocyte death by a constitutively active STAT3 in $FXR^{-/-}$ livers. A, Immunoblot analysis of ectopic STAT3 expression and real-time PCR analysis of STAT3 target gene Bcl-xl. Total protein extracts (30 μg) were pooled from livers of four mice that were hydrodynamically injected with constitutively active STAT3 (STAT3C). Liver samples were harvested 24 h after CCl_4 injections. Blots were probed with anti-flag antibody. Vector indicates the mice injected with the pCMV/Rc plasmid without insertion of STAT3C sequence; W/O indicates the mice with mock saline injection. B and C, Serum ALT (B) and BAs (C) levels in the indicated groups of $FXR^{-/-}$ mice. *, $P < 0.05$. D, Quantification of terminal deoxynucleotide transferase-mediated dUTP nick end labeling (TUNEL)-positive cells in randomly chosen fields. *, $P < 0.05$. E, Representative TUNEL-stained liver sections. F, Representative H&E-stained liver sections. *Arrows* indicate necrosis areas.

in CCl_4 treatment. Indeed, an exogenous supplement of BAs suppresses STAT3 phosphorylation in 70% PH livers. It is well known that cholestatic livers have impaired liver regeneration and display higher grades of liver injury (39). A previous study reported that BA treatment on rat hepatocytes *in vitro* can inhibit IL-6-induced STAT3 phosphorylation via a gp130- and p38α-dependent manner (30). However, we did not observe the similar mechanisms in our $FXR^{-/-}$ mouse models or 1% CA-containing diet models of cholestasis. This is potentially because the dose of the hydrophobic BA (GCDCA) that the two groups used *in vitro*, 100 μM, was not easily achieved in our cholestasis models. In contrast, we observed that high levels of BAs would directly modulate phosphorylation of JAK1 and JAK2, two direct upstream components of STAT3 and well-accepted main transducers of STAT3 pathways in liver regeneration (40). Our results thus indicate that the interference with STAT3 activation by high levels of BAs in damaged liver contributes to the defective liver repair. It should be mentioned that loss of other IL-6 family cytokines, such as IL-11, oncostatin M, leukemia inhibitory factor, and complement C3 may also be involved in the deficient STAT3 activation in the $FXR^{-/-}$ mice after CCl_4 treatment because of their documented roles in liver regeneration (41, 42).

Our previous studies suggest a novel role of FXR in promoting liver regeneration after 70% PH (17). However, there are intrinsic differences of responses between 70% PH and CCl_4-induced liver injury. In 70% PH, no significant apoptosis or necrosis is seen (17). In contrast, in CCl_4-induced injury, there is strong cell death and liver necrosis. The response of hepatocytes to cytokine pathways, such as STAT3 phosphorylation, in these two different types of liver damage is different also. Although the transient increase of BA will promote liver regeneration by activating FXR, it may aggravate liver injury after CCl_4 treatment. Therefore, we consider BA as a stress signal, and its function in liver repair depends on the status of FXR and the type of liver injury (43).

In summary, we demonstrate that FXR is essential to promote liver repair after injury. On one hand, FXR activation can directly transform the stress of BA overload into force of promotion of liver repair. For example, FXR promotes liver regeneration by regulating expression of genes involved in cell cycle progression such as *FoxM1b*. We also have evidence that *FoxM1b* is a FXR direct target gene (44). Therefore, FXR may direct a program of gene expression to promote liver regeneration after injury. On the other hand, FXR activation will help release the BA overload in liver, which can prevent BA-induced cell deaths and other deleterious effects on normal liver repair pathways such as STAT3 signaling. We propose that FXR is a novel liver protector (21). Therefore, FXR may represent a novel target of drug development to promote liver repair and to treat liver-injury related diseases.

Materials and Methods

Animal maintenance and treatments

Wild-type and $FXR^{-/-}$ mice were maintained as previously described (17). After an overnight fast, 8- to 12-wk-old mice were injected ip with a single dose of CCl_4 (750 μl/kg in corn oil) or vehicle control as the zero time point. All procedures followed the National Institute of Health guidelines for the care and use of laboratory animals. The cholestyramine or the cholic acid feedings are described previously (17).

RNA preparation and quantitative real-time PCR

RNA preparation was described previously (22). mRNA was quantified by real-time quantitative PCR using an Applied Biosystems 7300 Fast Real-Time PCR System (Applied Biosystems, Foster City, CA). The sequences of primers for each gene are provided in Supplemental Table 1.

EMSAs

Liver nuclear extract was prepared as described previously (22). Nuclear extracts (6 μg), polydeoxyinosinic deoxycytidylic acid (3 μg), and ^{32}P-radiolabeled oligonucleotides were coincubated for 30 min and separated by electrophoresis. For signal transducer and activator of transcription (STAT) 3-DNA binding analysis, double-stranded radiolabeled oligonucleotide high-affinity serum inducible element (5′-ATCCTCCAGCATTTCCCGTAAATCCTC-3′) was added to the mixture. The mixture was subjected to 5% nondenaturing gel electrophoresis. The gel was dried on chromatography paper (Whatman, Florham Park, NJ) and exposed overnight at −80 C using BioMax MS film (Eastman Kodak, Rochester, NY).

Western blotting

Liver total protein was prepared and separated as described previously (22). After blocking in 5% nonfat milk, the membranes were exposed to specific primary antibodies [anti-STAT3, anti-p65, antiphospho-STAT3-tyrosine 705, anti-p38α, antiphospho-p38α, anti-JAK1, antiphospho-JAK1, anti-JAK2, antiphospho-JAK2, and anti-cleaved Caspase 3 were from Cell Signaling Technology (Beverly, MA); anti-gp130 were from Santa Cruz Biotechnology, Inc. (Santa Cruz, CA); anti-flag and anti-β-actin were from Sigma (St. Louis, MO) at a concentration of 1:1000]. Membranes were then washed and exposed to peroxidase-conjugated secondary antibodies (Amersham Bioscience, Little Chalfont, Buckinghamshire, UK). Immunoblots were imaged using a medical film processor (SRX-101A; Konica Minolta Medical & Graphic Inc., New York, NY).

Adenovirus injection

Adenovirus expressing FXR-VP16 or VP16 alone was prepared and purified as previously described (22). Eight days after tail vein injection with 1×10^9 plaque-forming units of the FXR-VP16 adenovirus or the control per mouse, the mice were euthanized. Livers and blood were collected for analysis.

Primary hepatocyte preparation

Primary hepatocytes were isolated and cultured as described previously (22). GW4064 (2 μM) (TOCRIS Bioscience, Ellisville, MO) was applied to the hepatocytes, and 24 h later 10 ng/ml mouse recombinant IL-6 (PeproTech, Rocky Hill, NJ) was used to induce STAT3 phosphorylation.

Hydrodynamic injection

The pRc/CMV-stat3C-flag and pRc/CMV plasmid vectors, as described previously (45), were transfected into 8-wk-old male FXR mice via hydrodynamic injection through the tail vein, as described previously (32). The volume of the plasmid solutions was 0.1 ml/g body weight with a concentration of 10 μg/ml. the mice were injected with CCl_4 1 d after the infusion of the plasmids. Mice were euthanized and livers were removed for analysis 24 h later.

BA and serum ALT analysis

Total BAs were measured using the BA L3K assay kit, according to the manufacturer's instructions (Diagnostic Chemicals Limited, Oxford, CT). Serum ALT was measured at the City of Hope Helford Research Hospital.

Statistical analysis

Data are expressed as means ± SD. Two-tailed Student's *t* test was used to determine differences between data groups. $P < 0.05$ was considered statistically significant, unless otherwise stated.

Acknowledgments

We thank Dr. Keely Walker at City of Hope for her help in proofreading the manuscript. We thank Dr. Hua Yu at City of Hope for kindly providing the constitutively active STAT3 construct and Dr. Peter A. Edwards (University of California, Los Angeles, CA) for providing adenovirus that expressed VP16 alone (Ad-VP16) or murine FXRα2 fused to VP16 (FXR-VP16).

Address all correspondence and requests for reprints to: Wendong Huang, Ph.D, Department of Gene Regulation and Drug Discovery, Beckman Research Institute, City of Hope National Medical Center, 1500 East Duarte Road, Duarte, California 91010. E-mail: whuang@coh.org.

W.H. is supported by the Pilot/Feasibility Grant P30DK48522 from the University of Southern California Research Center for Liver Diseases and Concern Foundation.

Current address for N.L.: Department of Hematology and Oncology, First Affiliated Hospital of Jilin University, 71 Xinmin Street, Changchun City, Jilin 130041, China.

Disclosure Summary: The authors do not have any conflict of interest in this work.

References

1. **Forman BM, Goode E, Chen J, Oro AE, Bradley DJ, Perlmann T, Noonan DJ, Burka LT, McMorris T, Lamph WW, Evans RM, Weinberger C** 1995 Identification of a nuclear receptor that is activated by farnesol metabolites. Cell 81:687–693
2. **Makishima M, Okamoto AY, Repa JJ, Tu H, Learned RM, Luk A, Hull MV, Lustig KD, Mangelsdorf DJ, Shan B** 1999 Identification of a nuclear receptor for bile acids. Science 284:1362–1365
3. **Parks DJ, Blanchard SG, Bledsoe RK, Chandra G, Consler TG, Kliewer SA, Stimmel JB, Willson TM, Zavacki AM, Moore DD, Lehmann JM** 1999 Bile acids: natural ligands for an orphan nuclear receptor. Science 284:1365–1368
4. **Wang H, Chen J, Hollister K, Sowers LC, Forman BM** 1999 Endogenous bile acids are ligands for the nuclear receptor FXR/BAR. Mol Cell 3:543–553

5. **Goodwin B, Jones SA, Price RR, Watson MA, McKee DD, Moore LB, Galardi C, Wilson JG, Lewis MC, Roth ME, Maloney PR, Willson TM, Kliewer SA** 2000 A regulatory cascade of the nuclear receptors FXR, SHP-1, and LRH-1 represses bile acid biosynthesis. Mol Cell 6:517–526
6. **Lu TT, Makishima M, Repa JJ, Schoonjans K, Kerr TA, Auwerx J, Mangelsdorf DJ** 2000 Molecular basis for feedback regulation of bile acid synthesis by nuclear receptors. Mol Cell 6:507–515
7. **Wang YD, Chen WD, Huang W** 2008 FXR, a target for different diseases. Histol Histopathol 23:621–627
8. **Russell DW** 2003 The enzymes, regulation, and genetics of bile acid synthesis. Annu Rev Biochem 72:137–174
9. **Van Mil SW, Milona A, Dixon PH, Mullenbach R, Geenes VL, Chambers J, Shevchuk V, Moore GE, Lammert F, Glantz AG, Mattsson LA, Whittaker J, Parker MG, White R, Williamson C** 2007 Functional variants of the central bile acid sensor FXR identified in intrahepatic cholestasis of pregnancy. Gastroenterology 133:507–516
10. **Chen F, Ananthanarayanan M, Emre S, Neimark E, Bull LN, Knisely AS, Strautnieks SS, Thompson RJ, Magid MS, Gordon R, Balasubramanian N, Suchy FJ, Shneider BL** 2004 Progressive familial intrahepatic cholestasis, type 1, is associated with decreased farnesoid X receptor activity. Gastroenterology 126: 756–764
11. **Strautnieks SS, Bull LN, Knisely AS, Kocoshis SA, Dahl N, Arnell H, Sokal E, Dahan K, Childs S, Ling V, Tanner MS, Kagalwalla AF, Németh A, Pawlowska J, Baker A, Mieli-Vergani G, Freimer NB, Gardiner RM, Thompson RJ** 1998 A gene encoding a liver-specific ABC transporter is mutated in progressive familial intrahepatic cholestasis. Nat Genet 20:233–238
12. **van Mil SW, van der Woerd WL, van der Brugge G, Sturm E, Jansen PL, Bull LN, van den Berg IE, Berger R, Houwen RH, Klomp LW** 2004 Benign recurrent intrahepatic cholestasis type 2 is caused by mutations in ABCB11. Gastroenterology 127: 379–384
13. **Fiorucci S, Antonelli E, Rizzo G, Renga B, Mencarelli A, Riccardi L, Orlandi S, Pellicciari R, Morelli A** 2004 The nuclear receptor SHP mediates inhibition of hepatic stellate cells by FXR and protects against liver fibrosis. Gastroenterology 127:1497–1512
14. **Liu Y, Binz J, Numerick MJ, Dennis S, Luo G, Desai B, MacKenzie KI, Mansfield TA, Kliewer SA, Goodwin B, Jones SA** 2003 Hepatoprotection by the farnesoid X receptor agonist GW4064 in rat models of intra- and extrahepatic cholestasis. J Clin Invest 112: 1678–1687
15. **Park YJ, Qatanani M, Chua SS, LaRey JL, Johnson SA, Watanabe M, Moore DD, Lee YK** 2008 Loss of orphan receptor small heterodimer partner sensitizes mice to liver injury from obstructive cholestasis. Hepatology 47:1578–1586
16. **Cui YJ, Aleksunes LM, Tanaka Y, Goedken MJ, Klaassen CD** 2009 Compensatory induction of liver efflux transporters in response to ANIT-induced liver injury is impaired in FXR-null mice. Toxicol Sci 110:47–60
17. **Huang W, Ma K, Zhang J, Qatanani M, Cuvillier J, Liu J, Dong B, Huang X, Moore DD** 2006 Nuclear receptor-dependent bile acid signaling is required for normal liver regeneration. Science 312: 233–236
18. **Trudell JR, Bösterling B, Trevor AJ** 1982 Reductive metabolism of carbon tetrachloride by human cytochromes P-450 reconstituted in phospholipid vesicles: mass spectral identification of trichloromethyl radical bound to dioleoyl phosphatidylcholine. Proc Natl Acad Sci USA 79:2678–2682
19. **Yu C, Wang F, Jin C, Wu X, Chan WK, McKeehan WL** 2002 Increased carbon tetrachloride-induced liver injury and fibrosis in FGFR4-deficient mice. Am J Pathol 161:2003–2010
20. **Noé J, Stieger B, Meier PJ** 2002 Functional expression of the canalicular bile salt export pump of human liver. Gastroenterology 123:1659–1666
21. **Wang YD, Chen WD, Moore DD, Huang W** 2008 FXR: a metabolic regulator and cell protector. Cell Res 18:1087–1095
22. **Wang YD, Chen WD, Wang M, Yu D, Forman BM, Huang W** 2008 Farnesoid X receptor antagonizes nuclear factor κB in hepatic inflammatory response. Hepatology 48:1632–1643
23. **Fausto N, Campbell JS, Riehle KJ** 2006 Liver regeneration. Hepatology 43:S45–S53
24. **Ladu S, Calvisi DF, Conner EA, Farina M, Factor VM, Thorgeirsson SS** 2008 E2F1 inhibits c-Myc-driven apoptosis via PIK3CA/Akt/mTOR and COX-2 in a mouse model of human liver cancer. Gastroenterology 135:1322–1332
25. **Geier A, Kim SK, Gerloff T, Dietrich CG, Lammert F, Karpen SJ, Stieger B, Meier PJ, Matern S, Gartung C** 2002 Hepatobiliary organic anion transporters are differentially regulated in acute toxic liver injury induced by carbon tetrachloride. J Hepatol 37:198–205
26. **Bromberg JF, Wrzeszczynska MH, Devgan G, Zhao Y, Pestell RG, Albanese C, Darnell Jr JE** 1999 Stat3 as an oncogene. Cell 98:295–303
27. **Riehle KJ, Campbell JS, McMahan RS, Johnson MM, Beyer RP, Bammler TK, Fausto N** 2008 Regulation of liver regeneration and hepatocarcinogenesis by suppressor of cytokine signaling 3. J Exp Med 205:91–103
28. **Wang YD, Yang F, Chen WD, Huang X, Lai L, Forman BM, Huang W** 2008 Farnesoid X receptor protects liver cells from apoptosis induced by serum deprivation *in vitro* and fasting *in vivo*. Mol Endocrinol 22:1622–1632
29. **Huang YH, Chuang JH, Yang YL, Huang CC, Wu CL, Chen CL** 2009 Cholestasis downregulate hepcidin expression through inhibiting IL-6-induced phosphorylation of signal transducer and activator of transcription 3 signaling. Lab Invest 89:1128–1139
30. **Graf D, Kohlmann C, Haselow K, Gehrmann T, Bode JG, Häussinger D** 2006 Bile acids inhibit interleukin-6 signaling via gp130 receptor-dependent and -independent pathways in rat liver. Hepatology 44:1206–1217
31. **Yu H, Jove R** 2004 The STATs of cancer—new molecular targets come of age. Nat Rev Cancer 4:97–105
32. **Liu F, Song Y, Liu D** 1999 Hydrodynamics-based transfection in animals by systemic administration of plasmid DNA. Gene Ther 6:1258–1266
33. **Kim MS, Shigenaga J, Moser A, Feingold K, Grunfeld C** 2003 Repression of farnesoid X receptor during the acute phase response. J Biol Chem 278:8988–8995
34. **Xu G, Pan LX, Li H, Forman BM, Erickson SK, Shefer S, Bollineni J, Batta AK, Christie J, Wang TH, Michel J, Yang S, Tsai R, Lai L, Shimada K, Tint GS, Salen G** 2002 Regulation of the farnesoid X receptor (FXR) by bile acid flux in rabbits. J Biol Chem 277:50491–50496
35. **Zhang Q, He F, Kuruba R, Gao X, Wilson A, Li J, Billiar TR, Pitt BR, Xie W, Li S** 2008 FXR-mediated regulation of angiotensin type 2 receptor expression in vascular smooth muscle cells. Cardiovasc Res 77:560–569
36. **Greve JW, Gouma DJ, Buurman WA** 1989 Bile acids inhibit endotoxin-induced release of tumor necrosis factor by monocytes: an in vitro study. Hepatology 10:454–458
37. **Liu H, Lo CR, Jones BE, Pradhan Z, Srinivasan A, Valentino KL, Stockert RJ, Czaja MJ** 2000 Inhibition of c-Myc expression sensitizes hepatocytes to tumor necrosis factor-induced apoptosis and necrosis. J Biol Chem 275:40155–40162
38. **Dai G, He L, Bu P, Wan YJ** 2008 Pregnane X receptor is essential for normal progression of liver regeneration. Hepatology 47:1277–1287
39. **Yokoyama Y, Nagino M, Nimura Y** 2007 Mechanism of impaired hepatic regeneration in cholestatic liver. J Hepatobiliary Pancreat Surg 14:159–166

40. **Gao B** 2005 Cytokines, STATs and liver disease. Cell Mol Immunol 2:92–100
41. **Nakamura K, Nonaka H, Saito H, Tanaka M, Miyajima A** 2004 Hepatocyte proliferation and tissue remodeling is impaired after liver injury in oncostatin M receptor knockout mice. Hepatology 39:635–644
42. **Omori N, Evarts RP, Omori M, Hu Z, Marsden ER, Thorgeirsson SS** 1996 Expression of leukemia inhibitory factor and its receptor during liver regeneration in the adult rat. Lab Invest 75: 15–24
43. **Zhang L, Huang X, Meng Z, Dong B, Shiah S, Moore DD, Huang W** 2009 Significance and mechanism of CYP7a1 gene regulation during the acute phase of liver regeneration. Mol Endocrinol 23: 137–145
44. **Chen WD, Wang YD, Zhang L, Shiah S, Wang M, Yang F, Yu D, Forman BM, Huang W** 22 October, 2009 Farnesoid X receptor alleviates age-related proliferation defects in regenerating mouse livers by activating forkhead box m1b transcription. Hepatology 10.1002/hep23390
45. **Niu G, Wright KL, Huang M, Song L, Haura E, Turkson J, Zhang S, Wang T, Sinibaldi D, Coppola D, Heller R, Ellis LM, Karras J, Bromberg J, Pardoll D, Jove R, Yu H** 2002 Constitutive Stat3 activity up-regulates VEGF expression and tumor angiogenesis. Oncogene 21:2000–2008